PCCP

Accepted Manuscript




ROYAL SOCIETY OF CHEMISTRY

www.rsc.org/pccp

Journal Name

RSCPublishing

COMMUNICATION

# Hole-Transport Materials with Greatly-differing Redox Potentials give Efficient $TiO_2$-$[CH_3NH_3][PbX_3]$ Perovskite Solar Cells

Cite this: DOI: 10.1039/xoxxoooooox

Received ooth January 2012,
Accepted ooth January 2012

DOI: 10.1039/xoxxoooooox

www.rsc.org/

Antonio Abate,‡[b] Miquel Planells,‡[a] Derek J. Hollman,[b] Vishal Barthi,[c] Suresh Chand,[c] Henry J. Snaith[b]* and Neil Robertson[a]*

**Two diacetylide-triphenylamine hole-transport materials (HTM) with varying redox potential have been applied in planar junction $TiO_2$-$[CH_3NH_3]PbI_{3-x}Cl_x$ solar cells leading to high power-conversion efficiencies up to 8.8%. More positive oxidation potential of the HTM gives higher $V_{OC}$ and lower $J_{SC}$ illustrating the role of matching energy levels, however both HTMs gave efficient cells despite a difference of 0.44 V in their redox potentials.**

The recent development of lead halide perovskite based solar cells has led to a step change in the efficiencies of solution-processable solar cells culminating recently in certified power-conversion efficiencies reaching the range 16 – 18%.[1] The exceptional performance of these devices has been attributed to key properties of the perovskite layer including excellent electron and exciton mobility and direct band gap of appropriate energy for visible light harvesting.[2]

To date, **Spiro-OMeTAD** has been most commonly used as the HTM in the highest efficiency cells, however this material requires an expensive multi-step synthesis and shows hole-transport too low to carry all generated current.[3,4] In response, there has been increased recent interest in developing new HTMs aimed at addressing these limitations.[3-12] This work has explored alternative HTM structures, in particular based on the triarylamine and carbazole motifs,[6-11] leading to impressive power-conversion efficiencies (PCE) reaching around 14%.[6] In general however, these studies have paid limited attention to the exact redox properties of the new HTM provided the value lay approximately close to **Spiro-OMeTAD**, despite the fact that this molecule was designed for OLEDs and employed in solid-state dye-sensitised solar cells (ssDSSC) rather than perovskite cells.

Our recent work has led to a new diacetylide-triphenylamine (DATPA) series of HTMs,[13] prepared by a simple synthetic route, which in turn allows much easier tuning of electrochemical and other properties through varying the substituent R groups. These were studied as HTMs in ssDSSC and showed promising properties in comparison with **Spiro-OMeTAD**, with the key difference being the differing redox potentials. In this work, we now report a new dimethyl amino substituted HTM (**$Me_2N$-DATPA**) with very low first oxidation potential. We have used this, and our previously-reported (in the context of ssDSSC) **MeO-DATPA,** to prepare planar-junction $TiO_2$-$[CH_3NH_3]PbI_{3-x}Cl_x$ solar cells, the first perovskite cells that use the DATPA HTM series. This represents the first study specifically showing the effect of varying redox potential of structurally-similar HTMs on cell performance parameters.

The new **$Me_2N$-DATPA** molecule (Fig. 1*a*) was synthesised by a similar route to that we already reported for **MeO-DATPA**.[13] This involved Ullmann coupling to form the triarylamine fragment, followed by Sonogashira coupling to add a trimethylsilyl acetylide fragment and, after deprotection to remove the trimethylsilyl unit, a final oxidative homocoupling to form the central diacetylide unit (See ESI† for full details).

Single crystals suitable for X-Ray diffraction (XRD) were obtained by layer addition in EtOAc/DMSO. **$Me_2N$-DATPA** crystallised in the space group $P2_1/n$ and showed one molecule in the asymmetric unit (ESI†). The structure is arranged with the central diacetylide moieties approximately parallel between molecules. As expected the geometry around each triphenylamine is approximately planar and viewed along the long molecular axis, the molecules form herringbone arrangements that run in alternating directions. No intermolecular interactions are within Van der Waal radii, however the positioning of $Me_2N$- groups on the periphery of the molecule enables N…N contacts of 4.722 Å and 5.171 Å that link the molecules in a 2-D sheet (Fig. 2). Since the HOMO extends across the whole molecule including the peripheral nitrogen atoms (Fig 1*c*) such contacts can enhance effective hole transport within the material.

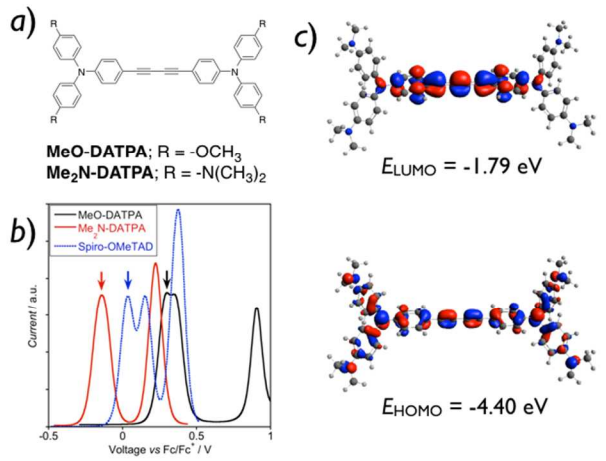


Fig. 1: *a*) Molecular structure of DATPA derivatives used in this study; *b*) Square-wave voltammetry (SWV) traces of the HTMs referenced to ferrocene. The arrow indicates the first oxidation potential from which $E_{HOMO}$ is derived and *c*) Molecular orbital distribution for **Me$_2$N-DATPA** at B3LYP/6-31G(d) level of theory (isodensity = 0.04). Absolute HOMO and LUMO energy values are experimentally obtained (see Table 1).

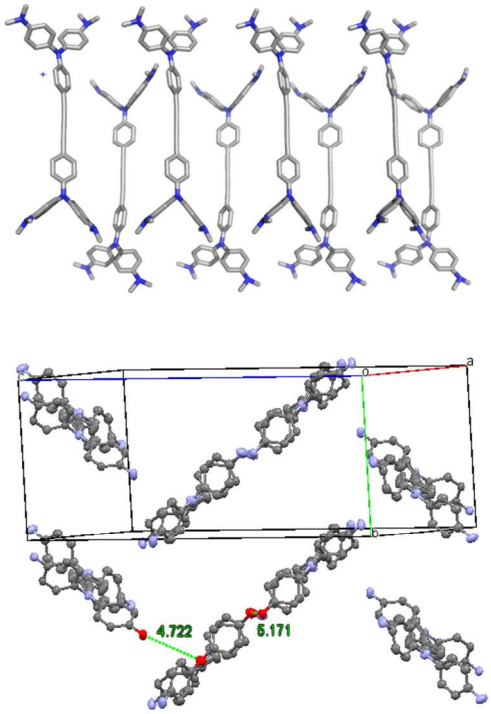


Fig. 2: Crystal structure of **Me$_2$N-DATPA** viewed along the short (upper) and long (lower) molecular axis. For clarity, methyl groups are removed in the lower view and short N…N contacts are indicated.

To assess the essential energy levels of **Me$_2$N-DATPA**, electrochemical analysis (cyclic and square-wave voltammetry) were performed to obtain the HOMO energy level. Spectroscopic methods (absorption and emission) were used to determine the gap and thus the LUMO energy level. Full details are given in ESI† and a summary of the resulting data given in Table 1 compared also with **Spiro-OMeTAD** and **MeO-DATPA**. Firstly, this confirmed little visible absorption by **Me$_2$N-DATPA**, in keeping with **MeO-DATPA** such that neither will significantly compete with the perovskite layer in the solar cell for light harvesting. The three HTMs differ markedly however in first oxidation potential, with that of **Me$_2$N-DATPA** being 0.44 V less positive than **MeO-DATPA** and 0.17 V less positive than **Spiro-OMeTAD** (Fig. 1*b*). This makes the new **Me$_2$N-DATPA** HTM a significantly stronger donor molecule (i.e. stronger hole acceptor) than either of the other two HTMs used to prepare the solar cells.

These observations were generally reinforced by calculations at the B3LYP/6-31G(d) level of theory with C-PCM in $CH_2Cl_2$, which showed a difference in HOMO energy levels of around 0.3 eV between **Me$_2$N-** and **MeO-DATPA**. The delocalisation of the HOMO onto the peripheral substituents (Fig 1*c*) explains the large shift in oxidation potential upon changing from MeO- to $Me_2N$-, and also favours the strong interactions between HOMOs of adjacent molecules required for effective hole transport.

Table 1. Summary of optical and electrochemical properties of HTM used in this study acquired in $CH_2Cl_2$ solution.

| HTM | $\lambda_{max}$ / nm | $\lambda_{em}$ / nm[b] | $E_{gap}$ / eV[c] | $E_{OX}$ / V[d] | $E_{HOMO}$ / eV[e] | $E_{LUMO}$ / eV[f] |
|---|---|---|---|---|---|---|
| **MeO-DATPA**[a] | 389 | 490 | 2.86 | +0.30 | –5.02 | –2.29 |
| **Spiro-OMeTAD**[a] | 385 | 424 | 3.05 | +0.03 | –4.64 | –2.16 |
| **MeN$_2$-DATPA** | 402 | 630 | 2.61 | –0.14 | –4.40 | –1.79 |

[a]Data from our previous work.[13] [b]Excitation at $\lambda_{max}$. [c]From the intersection of absorption and emission spectra. [d]From SWV and CV measurements and referenced internally to ferrocene. [e]$E_{HOMO}$ (eV) = –1.4 $E_{OX}$ (V) – 4.6.[14] [f]$E_{LUMO} = E_{HOMO} + E_{gap}$

To assess the hole-transport properties, a space-charge limited current (SCLC) method was used according to the methodology reported in detail in ESI† (Fig. 3, Fig. S4).[13] This involved a spin-coated layer of the HTM on an ITO/PEDOT-PSS substrate, followed by an evaporated gold counter electrode. Since the ITO and gold work functions are close to the HTM HOMO level, this creates a hole-only device from which the mobility can be determined. This led to a room-temperature value of 1.2 x $10^{-5}$ $cm^2V^{-1}s^{-1}$ for **Me$_2$N-DATPA** and lower values at reduced temperature, in keeping with a thermally-activated process. In comparison with our previously-reported value of 6.0 x $10^{-6}$ $cm^2V^{-1}s^{-1}$ for **MeO-DAPTA** under the same conditions, the slightly higher mobility for the new HTM may arise from N…N interactions involving the peripheral $Me_2N$ groups of the former as shown in Fig. 2. Overall however, the two values differ by only a factor of two and it seems likely that the significantly altered redox potential will play a larger role in solar cell performance.

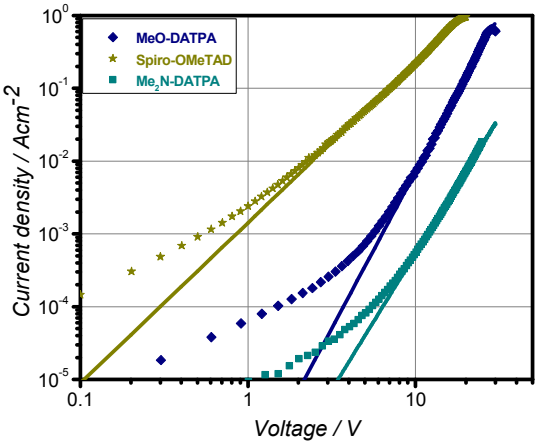


Fig. 3: *J–V* data for SCLC method of hole-mobility determination.

We prepared perovskite solar cells in keeping with previously reported methods and as described in detail in ESI†. DATPA derivatives and **Spiro-OMeTAD** were doped with protic ionic liquids following the method similar to that previously published[15] and as described more in detail in ESI†. All cells were prepared in a single continuous study using identical methods over 20 repeat cells for each HTM, enabling reliable comparison between the DATPA HTMs and **Spiro-OMeTAD** (Fig. 4 and Table 2). The latter showed the highest power-conversion efficiency (PCE) of 12.6%, however the corresponding values of 8.8% and 8.0% for **MeO-** and **$Me_2N$-DATPA** respectively are remarkably high for the first studies of new HTMs, given that **Spiro-OMeTAD** has undergone extensive optimisation of the doping and processing procedures over many years.

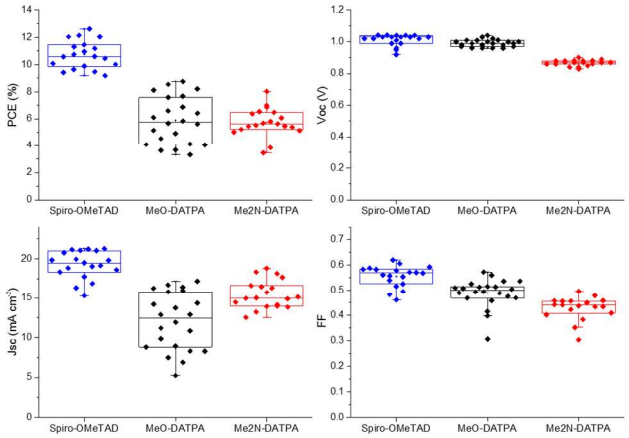


Fig. 4: Solar cell parameters over 20 repeats for each HTM.

Although the overall PCEs for the DATPA HTMs are similar, consideration of their $V_{OC}$ and $J_{SC}$ values reveals different origins to their respective performance. The average $J_{SC}$ is increased by 2.5 mAcm$^{-2}$ in changing from the weaker electron donor **MeO-DATPA** to the stronger **$Me_2N$-DATPA** indicating that the ability of the hole to be transferred efficiently to the HTM plays a crucial role in these cells. On the other hand, the HOMO level of **$Me_2N$-DATPA** is closer to vacuum, expected to lead to a smaller splitting of the quasi Fermi levels upon illumination between the $TiO_2$ and the HTM and this leads to the smaller $V_{OC}$ for the latter.

Table 2: Summary of solar cell performance showing best and average PCE for each HTM, along with related parameters.

| **HTM** | $V_{OC}$/ mV | $J_{SC}$/mA cm$^{-2}$ | ff | PCE/ % | μ/cm$^2$ V$^{-1}$s$^{-1}$ |
|---|---|---|---|---|---|
| Spiro-best | 1.03 | 21.24 | 0.58 | 12.6 | |
| Spiro-av | 1.03 ±0.03 | 19.52 ±1.75 | 0.57 ±0.04 | 10.6 ±1.0 | 3.6 x 10$^{-4}$ |
| MeO-best | 0.96 | 16.41 | 0.56 | 8.8 | |
| MeO-av | 0.99±0.02 | 12.40 ±3.64 | 0.50 ±0.06 | 5.9 ±1.7 | 6.0 x 10$^{-6}$ |
| $Me_2N$-best | 0.87 | 18.80 | 0.50 | 8.0 | |
| $Me_2N$-av | 0.87±0.02 | 14.99 ±1.82 | 0.44 ±0.04 | 5.7 ±1.1 | 1.2 x 10$^{-5}$ |

## Conclusions

We have prepared a new hole-transport material with a very strong hole-donor capability, adding to the redox-tunable series of substituted-DATPA HTMs we reported previously in the context of ssDSSC.[13] For the first time we have applied two DATPA molecules as the HTMs in perovskite solar cells leading to excellent efficiencies in both cases, despite the large difference in hole-donor strength. Close inspection indicates a trade-off in $V_{OC}$ with $J_{SC}$ as the HTM redox potential is changed, however the differences are perhaps not as great as might be expected; A 0.44 V difference in oxidation potential between the DATPA HTMs leads to only a 0.12 V difference in average $V_{OC}$ of the resulting cells. Likewise a difference in average $J_{SC}$ of only 2.5 mAcm$^{-2}$ is observed despite the 0.44 V difference in driving force for hole transfer. In contrast with solid or liquid-electrolyte dye-sensitised solar cells, this implies a wide tolerance of perovskite solar cells to function well with HTMs of greatly differing redox potential, suggesting a wider palette of HTMs might be explored for the further development of these devices.

## Acknowledgements

We thank the EPSRC (APEX Project, EP/H040218/1) for financial support. We thank Dr. Gary Nichol, University of Edinburgh for the crystallographic data collection and refinement and the EaStCHEM computational facility for access.

## Notes and references

[a]EastChem School of Chemistry, Kings Buildings, University of Edinburgh, Edinburgh EH9 3JJ, UK.

[b]Department of Physics, University of Oxford, Oxford OX1 3PU, UK
[c]CSIR-National Physical Laboratory, Dr. K.S. Krishnan Marg, New Delhi-110012, India.

†Electronic Supplementary Information (ESI) available: [Synthesis of $Me_2N$-DATPA; details of characterisation methods and solar cell fabrication. Figures: cyclic and square-wave voltammetries, UV-Visible absorption and photoluminescence spectra, packing diagram for $Me_2N$-DATPA, J-V data for SCLC hole mobility at different temperatures. Crystallographic table]. See DOI: 10.1039/c000000x/

‡ These authors contributed equally.

1 H. Zhou, Q. Chen, G. Li, S. Luo, T-B. Song, H-S. Duan, Z. Hong, J. You, Y. Liu, Y. Yang, *Science*, 2014, **345**, 542; N. J. Jeon, J. H. Noh, Y. C. Kim, W. S. Yang, S. Ryu, S. I. Seok, *Nature Mat.,* 2014, **13**, 897
2. M. Grätzel, *Nature Mat.,* 2014, **13**, 838
3. B. Xu, E. Sheibani, P. Liu, J. Zhang, H. Tian, N. Vlachopoulos, G. Boschloo, L. Kloo, A. Hagfeldt, L. Sun, *Adv. Mater.*, 2014, DOI: 10.1002/adma.201402415
4. H. Zhang, Y. Shi, F. Yan, L. Wang, K. Wang, Y. Xing, Q. Dong, T. Ma, *Chem. Commun*., 2014, **50**, 5020
5. H. Choi, S. Paek, N. Lim, Y. H. Lee, M. K. Nazeeruddin, J. Ko, *Chem. Eur. J.,* 2014, **20**, 10894
6. H. Li, K. Fu, A. Hagfeldt, M. Grätzel, S. G. Mhaisalkar, A. C. Grimsdale, *Angew. Chem. Int. Ed. Eng*., 2014, **53**, 4085
7. T. Krishnamoorthy, F. Kunwu, P. P. Box, H. Li, T. M. Koh, W. L. Leong, S. Powar, A. Grimsdale, M. Grätzel, N. Mathews, S. G. Mhaisalkar, *J. Mater. Chem. A*., 2014, **2**, 6305
8. J. Wang, S. Wang, X. Li, L. Zhu, Q. Meng, Y. Xiao, D. Li, *Chem. Commun*., 2014, **50**, 5829
9. D. Bi, L. Yang, G. Boschloo, A. Hagfeldt, E. M. J. Johansson, *J. Phys. Chem. Lett*., 2013, **4**, 1532
10. S. Lv, L. Han, J. Xiao, L. Zhu, J. Shi, H. Wei, Y. Xu, J. Dong, X. Xu, D. Li, S. Wang, Y. Luo, Q. Meng, X. Li, *Chem. Commun*., 2014, **50**, 6931
11. P. Qin, S. Paek, M. I. Dar, N. Pellet, J. Ko, M. Grätzel, M. K. Nazeeruddin, *J. Am. Chem. Soc*. 2014, **136**, 8516
12. K. Do, H. Choi, K. Lim, H. Jo, J. W. Cho, M. K. Nazeeruddin, J. Ko, *Chem. Commun.,* 2014, **50**, 10971
13. M. Planells, A. Abate, D. J. Hollman, S. D. Stranks, V. Bharti, J. Gaur, D. Mohanty, S. Chand, H. J. Snaith, N. Robertson *J. Mater. Chem. A*., 2013, **1**, 6949
14 B. W. D'Andrade, S. Datta, S. R. Forrest, P. Djurovich, E. Polikarpov, M. E. Thompson, *Org. Electron*., 2005, **6**, 11
15 A. Abate, D. J. Hollman, J. Teuscher, S. Pathak, R. Avolio, G. D'Errico, G. Vitiello, S. Fantacci, H. J. Snaith, *J. Am. Chem. Soc.*, 2013, **135**, 13538



 

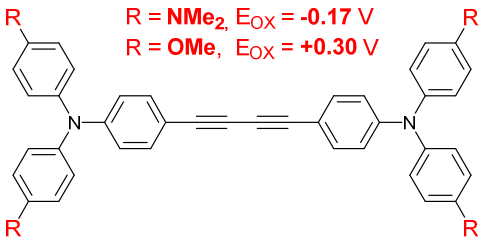


Hole-transport materials only 0.44 V different in redox potential give perovskite solar cells with only 0.12 V difference in $V_{OC}$ and similar PCEs.